# Photoinduced and redox-induced transmembrane processes with vesicle-stabilized colloidal cadmium sulfide and multicharged viologen derivatives

**ARTICLE** *in* THE JOURNAL OF PHYSICAL CHEMISTRY · APRIL 1991

Impact Factor: 2.78 · DOI: 10.1021/j100161a051



**3 AUTHORS**, INCLUDING:

Yves Tricot
Université de Fribourg
**21** PUBLICATIONS **480** CITATIONS
SEE PROFILE

Ze'ev Porat
Nuclear Research Center - Negev
**19** PUBLICATIONS **255** CITATIONS
SEE PROFILE

$$-\mathrm{d}\ln[Br_2^{\bullet-}]/\mathrm{d}t = k_{obs} = k_3k_4[SO_3^{2-}]/(k_{-3} + k_4)$$

If $k_4 \gg k_{-3}$, the reaction will behave as a simple bimolecular reaction. If, however, $k_{-3}$ is important, it can dramatically affect the kinetics and, particularly, decrease the activation energy. The more general case, in which the initial intermediate complex is in equilibrium with a secondary complex resulting from electron transfer, and in which the entire reaction is reversible, has been discussed before.[24] In that study, in which electron-transfer reactions between oppositely charged transition-metal complexes were investigated, activation energies less than that for diffusion were measured, even though the rate constants for the reactions were close to the diffusion-controlled limit.

There have been room temperature measurements of the rate constants for several of these reactions,[3] which generally agree with our $k_{298}$ values.[25] There have been a few studies of the temperature dependence for other radicals that we can discuss in light of the present results. The reaction of the stable free radical $ClO_2$ with the substitution-inert metal complex Co(terpy)$_2^{2+}$, which has a driving force of 0.67 V, was studied over the temperature range 5-30 °C and gives an activation energy of 18.6 kJ mol$^{-1}$.[11] This would lie slightly below the line we find for the oxidation of $W(CN)_8^{4-}$ and $Mo(CN)_8^{4-}$. The reaction of $O_3$ with $IrCl_6^{3-}$, studied from 4 to 34 °C, has an activation energy of 46.8 kJ mol$^{-1}$.[26] With a driving force of 0.12 V, this reaction lies slightly above the line extrapolated from the $Fe(CN)_6^{4-}$ results. In our earlier work,[4] we reported activation energies for a number of reactions of inorganic radicals with organic compounds. For reactions with driving forces above 0.4 V, the activation energies scatter below the lines presented here for the metal complexes. At lower driving force, the measured activation energies appear to increase sharply. The exception to this pattern is for the reactions of $NO_2$. This radical undergoes a large geometry change upon reduction,[11] possibly contributing to the higher activation energies for its reactions. The endothermic reaction of $ClO_2$ with $NO_2^-$, which has a driving force of -0.11 V, has an activation energy of 57.7 kJ mol$^{-1}$.[27] The reactions of $NO_2$ are probably not outer-sphere electron-transfer reactions. Indeed, the kinetic results on the reaction of $NO_2$ with $SO_3^{2-}$ were interpreted to suggest that $NO_2$ adds to $SO_3^{2-}$ to form a long-lived complex.[28]

In conclusion, the activation energies for the oxidation of the metal complexes by the various radicals are found to decrease with increasing exothermicity of the reaction. This is in line with an outer-sphere electron-transfer mechanism. On the other hand, we find little correlation of the activation energy with the driving force for the oxidation of the simple inorganic anions. Rather, variations in rate constants for these reactions are found to be, in some cases, more strongly dependent on changes in preexponential factors, which suggests that these reactions take place by an inner-sphere mechanism involving an intermediate adduct.

*Acknowledgment.* This research was supported by the Office of Basic Energy Sciences of the U.S. Department of Energy. L.C.T.S. was partly supported by the Indo-US collaborative program in material science. We thank Dr. G. Nahor for helpful discussion.

(24) Halpern, J.; Legare, R. J.; Lumry, R. *J. Am. Chem. Soc.* **1963**, *85*, 680.

(25) An exception is the recent work of: DeFelippis, M. R.; Murthy, C. P.; Faraggi, M.; Klapper, M. H. *Biochemistry* **1989**, *28*, 4847. They reported rate constants at room temperature for the oxidation of $ClO_2^-$ by $N_3^\bullet$ and $Br_2^{\bullet-}$ almost 40 times lower than we found by a similar technique and under similar conditions. They also reported a rate constant for the reaction of $(SCN)_2^{\bullet-}$ with $ClO_2^-$, whereas we found that $SCN^-$ reacted with $ClO_2$, so that we could not study this reaction. Our results, both here and in our earlier work (ref 12), are in line with the reactivity of $ClO_2^-$ toward other oxidants and its reactivity relative to the reactivity of $NO_2^-$.

(26) Bennett, L. E.; Warlop, P. *Inorg. Chem.* **1990**, *29*, 1975.

(27) Stanbury, D. M.; Martinez, R.; Tseng, E.; Miller, C. E. *Inorg. Chem.* **1988**, *27*, 4277.

(28) Clifton, C. L.; Altstein, N.; Huie, R. E. *Environ. Sci. Technol.* **1988**, *22*, 586.

# Photoinduced and Redox-Induced Transmembrane Processes with Vesicle-Stabilized Colloidal Cadmium Sulfide and Multicharged Viologen Derivatives

**Yves-M. Tricot,* Ze'ev Porat, and Joost Manassen**

*Department of Materials Research, The Weizmann Institute of Science, Rehovot 76100, Israel*
*(Received: February 28, 1990)*

Colloidal cadmium sulfide (CdS) and methylviologen ($MV^{2+}$) or new viologen derivatives carrying more positive charges were placed at specific sites of dihexadecyl phosphate (DHP) vesicles. Benzyl alcohol was used as a sacrificial electron donor to promote reduction of the viologens by photoexcited CdS colloid majority carriers. Transmission electron microscopy, $^{13}C$ nuclear magnetic resonance, and differential scanning calorimetry were used for physical characterization. Photochemical events were followed by in situ optical and electrochemical monitoring. Redox-induced transmembrane diffusion, which had been found with $MV^{2+}$, could be reduced by a factor 18 by using a triply charged viologen derivative and by a further factor of 30 in a configuration involving transmembrane electron transfer. In that case the quantum yield was ca. 0.05 at 410 nm, while virtually no reduced viologen leaking could be observed during at least 10 min. Physical evidence was found for a partial penetration of the CdS colloids into the DHP membrane.

## Introduction

Photochemical solar energy storage is a popular candidate as a possible source of alternative energy.[1] Despite substantial progress, its practical use is still restricted by energy-wasting back reactions. In natural photosynthesis, these reactions are avoided by use of lipid membranes carrying selectively located electron donors and acceptors. Attempts to re-create this scheme have been performed with various synthetic organized media. The models that most closely mimic biological membranes are planar bilayer lipid membranes (BLMs) and closed, unilamellar vesicles.[2,3]

* To whom correspondence should be addressed at Ilford AG, Industriestrasse 15, CH-1701 Fribourg, Switzerland.

(1) Fendler, J. H. *J. Phys. Chem.* **1985**, *89*, 2730.

(2) Tien, H. T. *Bilayer Lipid Membranes (BLM). Theory And Practice*; Marcel Dekker: New York, 1974.

(3) Hurst, J. K. In *Kinetics and Catalysis in Microheterogeneous Systems, Surfactant Science Series*; Marcel Dekker: New York, 1990.

0022-3654/91/2095-3242$02.50/0 

BLMs provide direct access to each side of the membrane and are ideally suited to study the mechanism of transmembrane processes. Unfortunately, their very small surface area makes product detection difficult and excludes use on a preparative scale. Vesicles, on the other hand, easily produce very large surface areas and, under the right conditions, remain stable for weeks or months. One cannot, however, directly access their interior. During preparation, reactants can be located selectively inside or outside the vesicles. However it is not usually known if the original configuration is maintained during illumination experiments. In particular, redox reactions taking place following transmembrane diffusion can be misinterpreted as true transmembrane electron transfer.[4,5]

We reported recently[6] the introduction of an in situ technique for separate monitoring of inner and outer photoproducts in vesicular media. This technique combined an optical absorbance measurement for the total concentration of the product with an electrochemical one to detect selectively the extravesicular fraction. Entrapped amounts were derived by difference. "Leaking" and transmembrane electron transfer could be clearly distinguished, and no a posteriori testing was necessary. The organized photoredox system was built from dihexadecyl phosphate (DHP) vesicles,[7,8] in situ generated colloidal CdS as photosensitizer, methylviologen ($MV^{2+}$) as electron acceptor, and benzyl alcohol as sacrificial electron donor.[9] This in situ technique revealed in the above system a high leaking rate for *reduced* $MV^{2+}$ ($MV^{\bullet+}$), while $MV^{2+}$ itself did not leak, even under illumination and in the presence of colloidal CdS. This phenomenon prevented the accumulation of reduced viologen inside the vesicles. Hurst et al.[10] also found independently that $MV^{\bullet+}$ was DHP membrane permeable, using chemical reduction techniques followed by spectroscopic examination. The more hydrophobic character of $MV^{\bullet+}$ compared to its parent dication could explain the ease of $MV^{\bullet+}$ leaking. We have therefore synthesized new viologen derivatives that carry one or two extra positive charges, keeping them more hydrophilic in their reduced form. This is, to our knowledge, the first use of such viologen derivatives: earlier works have mentioned the use of polymeric-type viologens[11] or viologens with extra *negative* charges[12] or added surfactant chains.[13] The result of our experiments confirmed the above assumption: one extra *positive* charge caused an 18-fold decrease of the leaking rate under the same geometrical conditions—photoreduction by coentrapped CdS colloids.[6] An additional 30-fold improvement was obtained if viologen reduction occurred after *transmembrane* electron transfer from *externally adsorbed* colloidal CdS. A virtually leakproof energy-storing system could be observed during at least 10 min of illumination.

## Experimental Section

*Sample Preparation and Characterization.* All commercial chemicals were of analytical grade and used as received, except methyl viologen dichloride, $MVCl_2 \cdot 2H_2O$ (Sigma), ruthenium tris(2,2′-bipyridine) dichloride, $Ru(bpy)_3Cl_2$ (Strem), anthracene-9-carboxylic acid (Aldrich, 98%), and argon (Matheson, 99.9%), which were purified as described in ref 6. Water was deionized and doubly distilled. Poly[*p*-xylyl-4,4′-bipyridine dibromide], $PXV\text{-}Br_2$ (polymeric viologen), was synthesized as described.[14] The preparation of new viologen derivatives with extra positive charges is described below.

**SCHEME I**

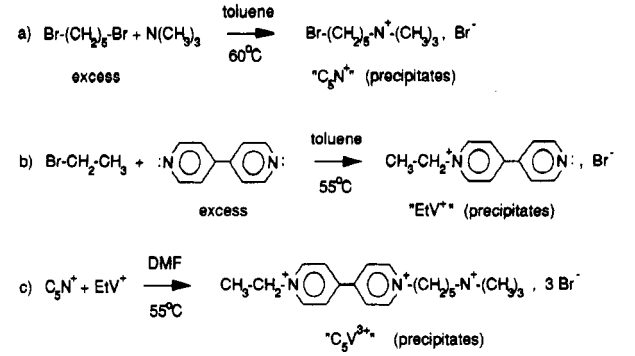


DHP vesicle dispersions containing CdS colloids and methylviologen on opposite or the same sides of the bilayer membrane were prepared following described procedures.[6] Sonication conditions were the same for methylviologen and the new viologen derivatives. However, modified techniques were necessary to remove the new viologens from outer vesicle surfaces. Instead of the cation exchange resin, which was sufficient for $MV^{2+}$, a $SiO_2$ column (BDH, 60–100 mesh, 30 × 300 mm) was used with the new compounds. The pH of the eluate was adjusted to 9.0 ± 0.1 by treatment of the column with 0.1 N KOH followed by flushing the column with distilled water. The elution rate was maintained at ca. 2 mL/min. The beginning and the end of the vesicle fraction were detected from the scattering of a small laser beam.[6] When present, outer $Cd^{2+}$ ions were also removed selectively by this treatment. Only the triply charged viologen could be selectively removed from outer vesicle surfaces by this treatment. The adsorption of the quadruply charged viologen or of the polymeric viologen was too strong. They could be removed by the $SiO_2$ column only at pH above 10, which also destroyed the vesicles.

Spectrophotometric characterization of the samples was done as described,[6] taking $\epsilon(257\text{ nm}) = 20\,700 \pm 200\ M^{-1}\ cm^{-1}$ for all oxidized viologen compounds and $\epsilon(633\text{ nm}) = 10\,800 \pm 500\ M^{-1}\ cm^{-1}$ for the reduced form. The wavelength of the monochromatic in situ optical detection system[6] (He–Ne laser) was 633 nm.

The oxygen-free electrochemical assembly, including reference, working, counter, and pH electrodes, as well as the illumination system, were as in the previous report.[6] The light source was a Sylvania tungsten–halogen, 15 V/150 W projector lamp, which was run at various voltages in the ranges 5–12 V (power ca. 20–90 W). The power was adjusted to obtain a similar viologen reduction rate for all the measured samples. It was a compromise between a reduction slow enough for the samples to remain homogeneous (correct electrochemical and optical responses) and fast enough to minimize the effect of competing reactions (reoxidation at the working electrode or because of traces of oxygen). Quantum yields were measured at 410 nm by using a monochromatic filter, from the initial part of the optical response due to viologen reduction. The adsorbed 410-nm photon flux was measured at several illumination intensities by in situ actinometry in the same electrochemical assembly, as described.[6] The absorbance of CdS colloids at 410 nm was corrected for the scattering of the vesicles.

Transmission electron micrograph (TEM) pictures were made on a JEOL JEM-70 instrument operated at 80 kV, with or without negative staining (uranyl acetate). Differential scanning calorimetry (DSC) measurements used a Mettler TA 3000 instrument. Nuclear magnetic resonance (NMR) spectra of synthesized compounds were recorded on a Varian CFT-20 spectrometer ($^1H$, 80 MHz) and on a Bruker WH-90 spectrometer ($^{13}C$, 22.6 MHz). $^{13}C$ NMR spectra of vesicle samples were recorded at 67.9 MHz on a Bruker WH-270 spectrometer.

*Preparation of Higher Charge Viologens.* To our knowledge, the synthesis of the following triply and quadruply charged

(4) Tunuli, M. S.; Fendler, J. H. *J. Am. Chem. Soc.* **1981**, *103*, 2507.
(5) Lee, L. Y. C.; Hurst, J. K.; Politi, M.; Kurihara, K.; Fendler, J. H. *J. Am. Chem. Soc.* **1983**, *105*, 370.
(6) Tricot, Y.-M.; Manassen, J. *J. Phys. Chem.* **1988**, *92*, 5239.
(7) Mortara, R. A.; Quina, F. H.; Chaimovich, H. *Biochem. Biophys. Res. Commun.* **1978**, *81*, 1080.
(8) Tricot, Y.-M.; Furlong, D. N.; Sasse, W. H. F.; Daivis, P.; Snook, I. *Aust. J. Chem.* **1983**, *36*, 609.
(9) Tricot, Y.-M.; Emerén, Å.; Fendler, J. H. *J. Phys. Chem.* **1985**, *89*, 4721.
(10) Patterson, B. C.; Thompson, D. H. P.; Hurst, J. K. *J. Am. Chem. Soc.* **1988**, *110*, 3656.
(11) Sassoon, R. E.; Gershuni, S.; Rabani, J. *J. Phys. Chem.* **1985**, *89*, 1937.
(12) Degani, Y.; Willner, I. *J. Am. Chem. Soc.* **1983**, *105*, 6228.
(13) Maidan, R.; Goren, Z.; Becker, J. Y.; Willner, I. *J. Am. Chem. Soc.* **1984**, *106*, 6217.
(14) Factor, A.; Heinsohn, G. E. *Polym. Lett.* **1971**, *9*, 289.

SCHEME II

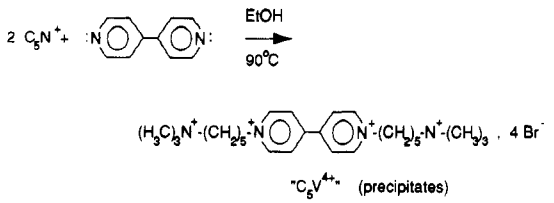


viologens has not been described. The preparation of several analogous viologen compounds has been mentioned, but without synthetic procedure.[15]

(1) *Synthesis of a Triply Charged Viologen.* The synthetic route is given in Scheme I.

*Preparation of* $C_5N^+$: 1,5-Dibromopentane (140 mmol, 32.2 g, 19.0 mL) was mixed with 50 mL of toluene in a 250-mL bottle at room temperature. Trimethylamine (35 mmol, 2070 mg) was dissolved in 10 mL of precooled toluene at 0 °C and rapidly added to the 1,5-dibromopentane solution. The bottle (250 mL) was quickly closed and heated to 60 °C under magnetic stirring for at least 10 h. The white precipitate of $C_5N^+$ was vacuum-filtered, washed with 10 mL of *cold* toluene and then three times with 10–15 mL of ether, and dried for an hour at 120 °C. Yield ca. 9.1 g or 90% of the trimethylamine. This product contained a small fraction of doubly reacted compound, which was eliminated by dispersion in DMF at 60–70 °C (ca. 25 mL of DMF for 9.1 g), filtration, and ether-induced recrystallization. Final yield ca. 6.8 g or 75% of the crude product. Anal. Calcd for $C_8H_{19}NBr_2$: C, 33.24; H, 6.63; N, 4.85; Br, 55.29. Found: C, 33.59; H, 6.52; N, 4.88; Br, 54.86. The structure was confirmed by $^{13}C$ and $^1H$ NMR analyses, which showed no visible impurities. Melting point 137–140 °C.

*Preparation of* $EtV^+$: 4,4'-Bipyridine (12 mmol, 1874 mg) was dissolved in 4 mL of toluene at 50–55 °C in a 25-mL vial. Ethyl bromide (4 mmol, 300 μL, 436 mg) was injected in the solution, and the vial was promptly closed and kept at 50–55 °C for ca. 10 h under magnetic stirring. The hygroscopic, cream-colored precipitate was vacuum-filtered under argon atmosphere. Toluene and excess 4,4'-bipyridine were removed by washing with ether. The product was dried under argon at 50 °C. Yield ca. 750 mg or 70% from ethyl bromide. No yellow, doubly reacted product was observed. Anal. Calcd for $C_{12}H_{13}N_2Br$: C, 54.36; H, 4.94; N, 10.57; Br, 30.14. Found: C, 53.23; H, 4.99; N, 10.35; Br, 25.92. The structure was confirmed by $^{13}C$ and $^1H$ NMR analyses, which revealed no significant impurities. Melting point 65–70 °C.

*Preparation of* $C_5V^{3+}$: $C_5N^+$ (2 mmol, 578 mg) was dispersed in 2 mL of dry DMF, heated to 55–60 °C, and added to 2 mmol (530 mg) of dry $EtV^+$ in a 20-mL vial under argon, and the vial was quickly closed. It was kept at 55 °C under magnetic stirring for ca. 10 h; a yellow precipitate started to form within a few hours. This product was extremely hygroscopic. Ether (15 mL) was added under argon to the thick yellow paste, and the product was stirred to get a light-yellow powder suspension. Ether was removed with a pipet, and fresh ether was added several times into the same vial to wash away DMF. The product was dried under argon at 50 °C. Yield: ca. 850 mg or 75% of $C_5N^+$. Anal. Calcd for $C_{20}H_{32}Br_3N_3$: C, 43.35; H, 5.82, N, 7.58; Br, 43.25. Found: C, 43.84; H, 6.23; N, 8.23; Br, 39.08. $^1H$ NMR (in TFA-*d* as solvent and internal standard at 15.84 ppm vs TMS) δ 9.26 (4 H, m), 8.72 (4 H, d, $J$ = 6.2 Hz), 5.00 (4 H, m), 3.63 (2 H, m), 3.30 (9 H, s), ca. 2.2 (6 H, br m), 1.92 (3 H, t, $J$ = 7.3 Hz); $^{13}C$ NMR (in $D_2O$, with TMS/$CDCl_3$ as external standard) δ 127.7, 126.5, 122.7, 53.4, 30.1, 22.3, 22.0, 15.9. A few small impurity peaks were visible (DMF and traces of starting material). The UV spectrum was the same as methylviologen. Melting point: 170–180 °C (dec).

(2) *Synthesis of a Quadruply Charged Viologen.* The synthetic route is given in Scheme II.

(15) Bird, C. L.; Kuhn, A. T. *Chem. Soc. Rev.* **1981**, *10*, 49.

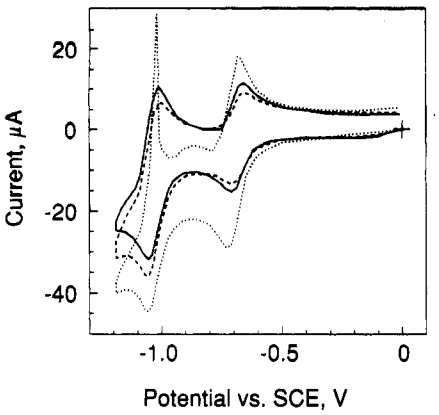


**Figure 1.** Cyclic voltammograms of $10^{-3}$ M viologens in 0.5 M KCl. Sweep rate, 100 mV/s; working electrode, glassy carbon. (···) $MV^{2+}$; (—) $C_5V^{3+}$; (---) $C_5V^{4+}$.

**TABLE I: Electrochemical Properties of $MV^{2+}$, $C_5V^{3+}$, $C_5V^{4+}$, and PXV-$Br_2$**

| viologen compd | cyclic voltammetry, V vs SCE | | WE in photochemical cell sensitivity to viologen radical[b] | |
|---|---|---|---|---|
| | $E^\circ_{1/2}(1)$ | $E^\circ_{1/2}(2)$ | current, A·$M^{-1}$ | $k_{reox}$,[c] $s^{-1}$ |
| $MV^{2+}$ | −0.700 | −1.040 | 3.80 | $5.26 \times 10^{-4}$ |
| $C_5V^{3+}$ | −0.687 | −1.035 | 0.54 | $7.99 \times 10^{-5}$ |
| $C_5V^{4+}$ | −0.680 | −1.032 | 0.12 | $1.77 \times 10^{-5}$ |
| PXV-$Br_2$ | −0.436[a] | −0.854[a] | 0.03 | $4.40 \times 10^{-6}$ |

[a] From ref 15, measured by polarography. [b] In the presence of $10^{-3}$ M DHP vesicles, with WE potential set at −0.32 V vs SCE, under constant stirring, with ca. $5 \times 10^{-5}$ M viologen concentration. [c] Apparent rate constant for reoxidation at the working electrode (WE), calculated with eq 3 (see Discussion).

*Preparation of* $C_5V^{4+}$: $C_5N^+$ (4 mmol, 1156 mg) was dissolved in 2 mL of dry EtOH at 60 °C and added to 2 mmol (312 mg) of 4,4'-bipyridine in a 25-mL vial. The vial was closed and heated to 90 °C, under magnetic stirring. The solution turned deep yellow, and after ca. 20 h, the product precipitated spontaneously or upon cooling to room temperature. $C_5V^{4+}$ was treated with ether as $C_5V^{3+}$ and then EtOH was removed. Yield after drying at 50 °C: ca. 1400 mg or 95%. Anal. Calcd. for $C_{26}H_{46}Br_4N_4$: C, 42.35; H, 6.31; N, 7.63; Br, 43.53. Found: C, 41.15; H, 6.41; N, 7.27; Br, 42.29. $^1H$ NMR (in TFA-*d* as solvent and internal standard at 15.84 ppm vs TMS) δ 9.31 (4 H, d, $J$ = 5.9 Hz), 8.72 (4 H, d, $J$ = 6.3 Hz), 5.00 (4 H, t, $J$ = 7.0 Hz), 3.67 (4 H, m), 3.30 (18 H, s), ca. 2.2 (8 H, br m); $^{13}C$ NMR (in $D_2O$, with TMS/$CDCl_3$ as external standard) δ 126.9, 125.9, 122.9, 53.0, 31.2, 29.9, 22.0, 21.6, 21.2. A few small impurity peaks were visible (solvent or decomposition products). The UV spectrum was the same as methylviologen. Melting point: 235–240 °C (dec).

## Results

*Electrochemical Comparison of the Viologens.* Figure 1 shows cyclic voltammograms (CV) of the three compounds in aqueous solutions. The potentials for the first and second reduction steps of $C_5V^{3+}$ and $C_5V^{4+}$ were 10–20 mV more positive than those of $MV^{2+}$ (Table I). More pronounced shifts have been reported for similar viologen derivatives having shorter side chains.[15] The sharp reoxidation peak visible in $MV^{2+}$ CV (Figure 1) was due to precipitation of the insoluble $MV^0$ at the electrode. $C_5V^{3+}$ and $C_5V^{4+}$ did not produce such peaks since they remained positively charged and therefore soluble even when fully reduced. Detailed CV studies have been performed with these compounds and are reported elsewhere.[16]

In the presence of negatively charged DHP vesicles, adsorption of the viologens reduced the electrochemical currents. This effect

(16) Porat, Z.; Zinger, B.; Tricot, Y.-M.; Rubinstein, I. *Proc. Electrochem. Soc. Meeting*, Montreal, 1990.

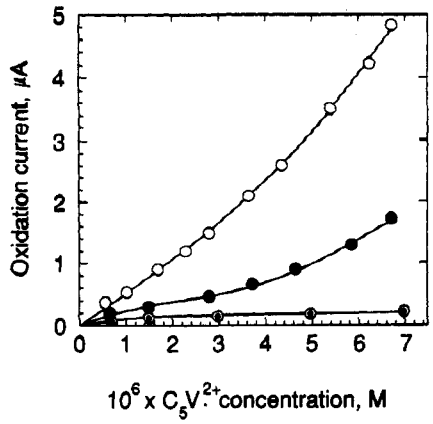


**Figure 2.** Correlation between the oxidation current of $C_5V^{\bullet 2+}$ and its concentration (determined from the absorbance at 633 nm) during visible-light irradiation of $5 \times 10^{-5}$ M CdS colloids and $2 \times 10^{-5}$ M $C_5V^{3+}$ in $10^{3+}$ in $10^{-3}$ M DHP vesicles with 0.1 vol % benzyl alcohol at pH 7. (○) CdS and $C_5V^{3+}$ at the outer surface of the vesicles; (●) CdS and $C_5V^{3+}$ at the inner surface of the vesicles; (⊙) CdS at the outer and $C_5V^{3+}$ at the inner surface of the vesicles.

had been previously observed with $MV^{2+}$ and other doubly charged viologens[17] and was markedly stronger with $C_5V^{3+}$, $C_5V^{4+}$, and the poly(xylylviologen) (PXV-$Br_2$). The relative sensitivities of the one-electron-reduced viologens at the working electrode in illumination experiments are given in Table I. In these experiments, the viologens were photoreduced at the outer vesicle surfaces by conduction-band electrons of CdS colloids also present outside the vesicles. For entrapment experiments, we used $C_5V^{3+}$ since it was the only multicharged viologen that could be selectively located inside the vesicles. Its electrochemical detection was also much easier than that of reduced $C_5V^{4+}$.

*Control of Redox-Induced Transmembrane Diffusion.* Two different configurations were investigated: one had CdS colloids *and* $C_5V^{3+}$ *inside* the vesicles, and the other had CdS colloids *outside* and $C_5V^{3+}$ *inside* the vesicles. Results of illumination experiments are shown in Figure 2 for these two configurations and for the calibration system (CdS colloids *and* $C_5V^{3+}$ *outside* the vesicles). Similar data were presented before[6] with $MV^{2+}$ instead of $C_5V^{3+}$. Each curve in Figure 2 is the average of at least three individual runs, reproducible within ca. 15%. The oxidation current measured at the working electrode was determined by the outer surface concentration of reduced viologen. The total concentration of reduced viologen was measured spectroscopically and in situ by using the 633-nm laser beam (see Experimental Section). In the calibration configuration with CdS colloids and $C_5V^{3+}$ outside the vesicles, both the optical and electrochemical responses were time-independent and reversible, since the viologens were reduced and reoxidized on the same side of the vesicles (outside). On the other hand, when $C_5V^{3+}$ was reduced inside the vesicles, reoxidation nevertheless took place outside the vesicles—at the working electrode, following transmembrane diffusion. Once the viologens were reoxidized by the electrode, they could not return inside and the configuration was irreversibly modified. A more quantitative evaluation of these results will be presented in the Discussion.

Reduction of $C_5V^{3+}$ did not occur with the same efficiency in each configuration. The 410-nm quantum yields of viologen radical formation were measured by using $C_5V^{3+}$ and $MV^{2+}$ (and $C_5V^{4+}$ only at the outer vesicle surface), in the three above configurations (Table II). No significant quantum yield variation was found between the different viologens.

*Physical Characterization of Vesicle-Stabilized CdS Colloids.* It had been observed in an earlier work[18] that CdS colloids did not diffuse through the vesicle wall, but their exact location in the membrane remained unknown. Differential scanning calorimetry (DSC) was used to probe the interaction of CdS colloids with the vesicle bilayer. An increase of disorder of the membrane, as caused by the penetration of CdS colloids, would result in a lowering of phase transition temperatures. DSC thermograms are shown in Figure 3. Pure DHP (5 mg) was measured as a reference. The main melting peak was at ca. 82 °C, and the shoulder at ca. 78 °C was due to the solid-to-liquid-crystalline, or "chain-melting", transition. The vesicular samples were 30 μL of $2 \times 10^{-2}$ M DHP dispersions, containing only 0.33 mg of pure DHP, giving therefore smaller signals than the reference sample. The sharp peaks appearing in the vesicle DSC thermograms were artifacts due to sudden evaporation in the measured or the reference samples that occurred sometimes above 80 °C (the reference samples were 30 μL of $H_2O$). In vesicular form without CdS colloids, the chain-melting peak was however clearly resolved and shifted to ca. 72 °C, while the main melting peak was broader and slightly shifted to 80 °C. These shifts already indicated an increase of disorder from pure DHP material to vesicle dispersions. In the presence of $4 \times 10^{-3}$ M CdS colloids outside the vesicles, both peaks were further broadened, and the chain-melting peak was even further shifted. The latter peak disappeared completely in the presence of $6 \times 10^{-3}$ M CdS colloids on both sides of the vesicles. These effects suggested an increase of disorder in the bilayer structure with the presence of CdS colloids, due to the penetration of the colloids in the membrane. The results did not indicate how deeply the surfactant chains were disturbed. This information should be obtained from $^{13}C$ NMR, because the

**TABLE II: The 410-nm Quantum Yield of Viologen Reduction ($MV^{2+}$ or $C_5V^{3+}$, $C_5V^{4+}$ Only Outside) by Colloidal CdS in Various Vesicular Systems in the Presence of 0.1% Benzyl Alcohol as Electron Donor**

| configuration | quantum yield | presumed limiting factor |
|---|---|---|
| viologen outside, CdS outside | 0.4–0.6 | electron–hole recombination |
| viologen inside, CdS inside | 0.005–0.01 | transmembrane diffusion of benzyl alcohol |
| viologen inside, CdS outsie | 0.05–0.07 | transmembrane electron transfer |

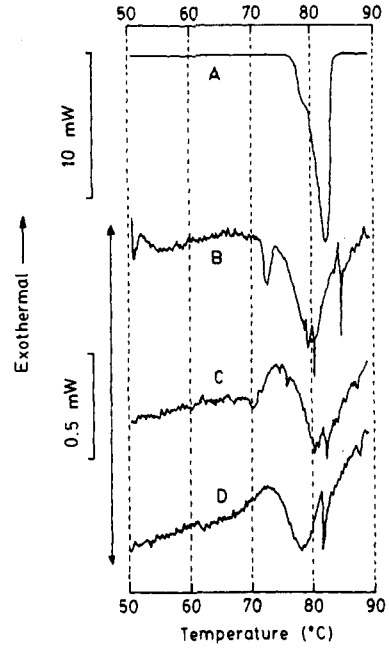


**Figure 3.** Differential scanning calorimetry at 2 °C/min of dihexadecyl phosphate (DHP) surfactant in various conditions: (A) 5 mg of pure DHP; (B) 30-μL $2 \times 10^{-2}$ M DHP vesicles (0.33 mg of DHP), without CdS colloids; (C) 30-μL $2 \times 10^{-2}$ M DHP vesicles with $4 \times 10^{-3}$ M CdS colloids at the outer surface of the vesicles; (D) 30-μL $2 \times 10^{-2}$ M DHP vesicles with $6 \times 10^{-3}$ M CdS colloids distributed at the inner and outer surfaces of the vesicles.

(17) Lu, T.; Cotton, T. M.; Hurst, J. K.; Thompson, D. H. P. *J. Electroanal. Chem.* **1988**, *246*, 337.
(18) Tricot, Y.-M.; Fendler, J. H. *J. Am. Chem. Soc.* **1984**, *106*, 7359.
(19) Tricot, Y.-M.; Fendler, J. H. *J. Phys. Chem.* **1986**, *90*, 3369.

**TABLE III: Effect of Colloidal CdS on $^{13}C$ NMR Line Widths of Dihexadecyl Phosphate (DHP) Carbons in the Vesicle Membrane ($2 \times 10^{-2}$ M DHP, 80 °C)**

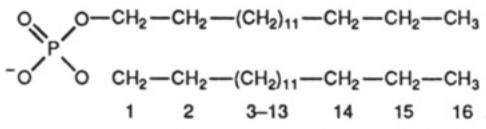


| configuration | line widths, Hz | | | | | |
|---|---|---|---|---|---|---|
| no CdS | 6 | 10 | 41 | 5 | 7 | 6 |
| $4 \times 10^{-3}$ M CdS outside | 12 | 13 | 49 | 6 | 6 | 5 |
| $6 \times 10^{-3}$ M CdS both sides | 10 | 26 | 62 | 7 | 7 | 6 |

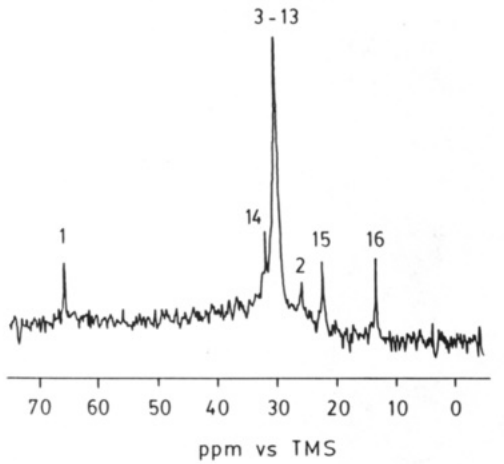


**Figure 4.** $^{13}C$ NMR spectrum at 67.9 MHz of $2 \times 10^{-2}$ M dihexadecyl phosphate (DHP) vesicles at 80 °C, in the absence of CdS colloids. The carbon number assignment and the measured line widths are given in Table III. The chemical shifts are relative to external TMS in $CDCl_3$ (with same $D_2O$ lock signal). Spectrum obtained after ca. 2000 scans (30-min accumulation time).

molecular motion restriction produced by the CdS colloid–membrane interaction would be expected to selectively broaden the $^{13}C$ NMR signals.[20] Below the chain-melting temperature, the $^{13}C$ NMR peaks of DHP vesicles without CdS colloids were already very broad. Measurements were done, therefore, at 80 °C. Figure 4 shows the $^{13}C$ NMR spectrum of $2 \times 10^{-2}$ M DHP in vesicles without CdS, at 80 °C. It is given to demonstrate the degree of selectivity of the technique for the observation of specific parts of the membrane. Differences between this spectrum and the ones recorded in the presence of CdS colloids were not directly visible unless each peak was strongly expanded. Peak line widths obtained from enlarged plots are listed in Table III, for spectra obtained without CdS and with CdS only inside or on both sides of the vesicles. It appeared that the hydrocarbon chain ends were not affected by the presence of the CdS colloids, unlike the polar end (carbons 1 and 2). The middle carbon seemed to be only weakly affected. Consequently, the penetration of the CdS colloids in the bilayer at 80 °C appeared to be restricted to the outer part of the membrane. At room temperature, even less penetration should be expected.

Further information was sought from transmission electron microscopy (TEM). A TEM picture of DHP-stabilized CdS colloids had been published earlier,[18] but it did not show clearly the CdS particles. In Figure 5 are presented TEM pictures of stained and unstained DHP vesicles samples with *outer surface* CdS colloids. The pictures show clearly the vesicles and the CdS colloids, some of them being clustered and appearing to be attached to the vesicle membrane. The unstained picture shows also a large fraction of loose CdS colloids. It was not possible to know from the TEM pictures whether these colloids were disconnected from

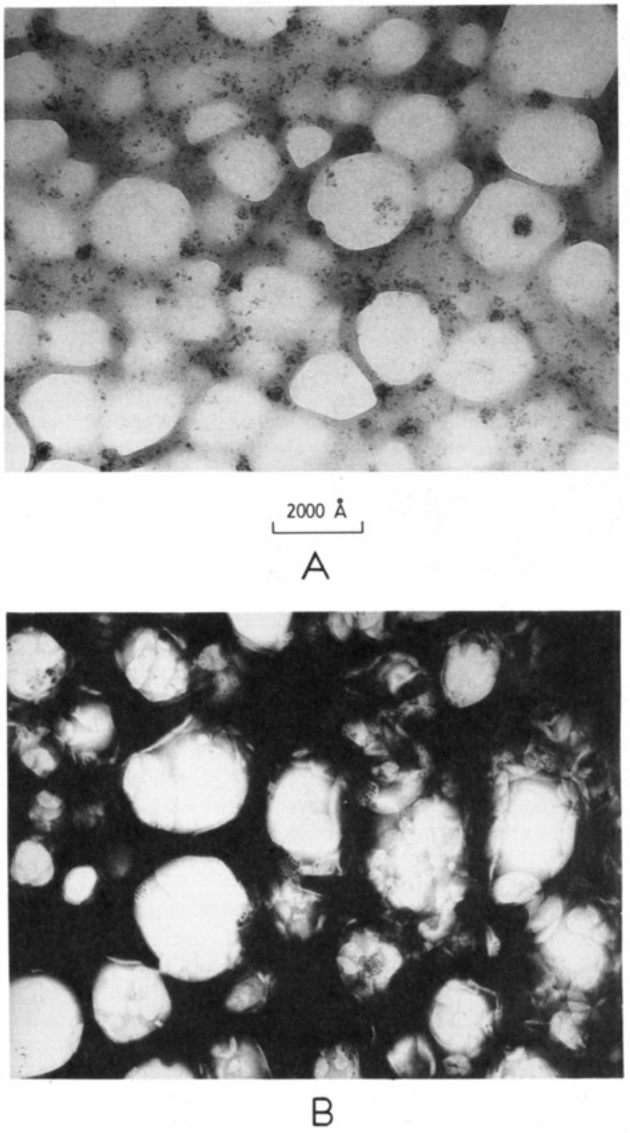


**Figure 5.** Transmission electron micrographs of dihexadecyl phosphate (DHP) vesicles and CdS colloids. Initial conditions: $2 \times 10^{-3}$ M DHP and $2 \times 10^{-4}$ M CdS colloids located at the outer surface of the vesicles: (A) unstained; (B) stained with uranyl acetate.

the vesicles during the preparation of the samples (drying on carbon grids) or if they were already free in solution. The vesicle diameters were in the range 500–2000 Å, in agreement with previous studies.[8] Similar pictures were obtained with CdS colloids on both sides of the vesicles. It was difficult to see the colloids if they were only inside, presumably because of their smaller size.[19]

## Discussion

*Transmembrane Diffusion Kinetics.* Viologen leaking kinetics were derived by using the same method applied previously[6] to $MV^{2+}$. The recorded oxidation currents were used to measure the fraction of reduced viologen that had leaked and had become accessible to the working electrode, by using the relation established from the calibration configuration (see Results). Derived kinetic curves for the system with *both* $C_5V^{3+}$ and CdS colloids initially inside the vesicles are shown in Figure 6. The similar results obtained with $C_5V^{3+}$ inside the CdS colloids outside are shown in Figure 7. As mentioned in the Experimental Section, different intensities were used with white-light illuminations in order to generate $C_5V^{\bullet 2+}$ with approximately the same rate in both configurations. Quantum yields are discussed below. The following model was used to evaluate the rate of $C_5V^{\bullet 2+}$ leaking:

$$[V^{n+}]_{in} \xrightarrow{k_{red}} [V^{(n-1)+}]_{in} \underset{k_{leak}^{-1}}{\overset{k_{leak}}{\rightleftharpoons}} [V^{(n-1)+}]_{out} \xrightarrow{k_{reox}} [V^{n+}]_{out} \qquad (1)$$

(20) Tricot, Y.-M.; Kiwi, J.; Niederberger, W.; Grätzel, M. *J. Phys. Chem.* **1981**, *85*, 862.

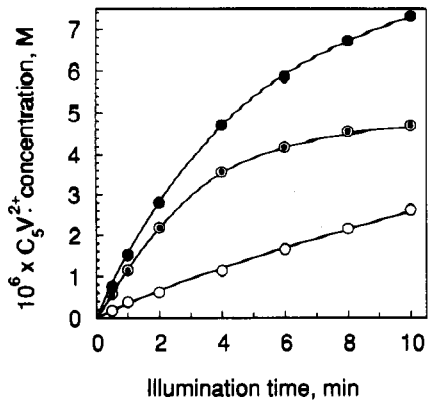


**Figure 6.** Dynamic evolution of $C_5V^{\bullet 2+}$ distribution under ca. 60-W visible-light irradiation of $6 \times 10^{-5}$ M CdS colloids and $5 \times 10^{-5}$ M $C_5V^{3+}$ *both entrapped* in $10^{-3}$ M DHP vesicles, in the presence of 0.1 vol % benzyl alcohol at pH 7. (●) total $C_5V^{\bullet 2+}$ concentration, measured in situ by absorbance at 633 nm; (○) outer surface $C_5V^{\bullet 2+}$ concentration, measured electrochemically; (⊙) inner surface $C_5V^{\bullet 2+}$ concentration, calculated from the total and outer surface concentrations (see text for details).

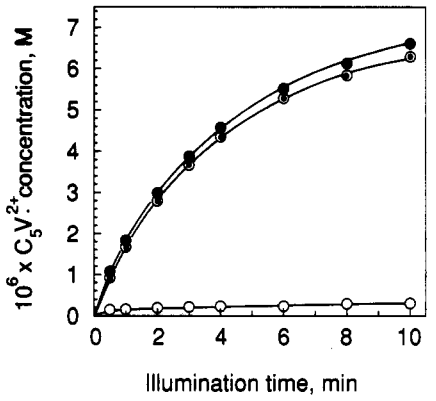


**Figure 7.** Accumulation of $C_5V^{\bullet 2+}$ inside $10^{-3}$ M DHP vesicles under ca. 20-W visible-light irradiation of $1.7 \times 10^{-4}$ M CdS colloids at the outer surface and $2.4 \times 10^{-5}$ M $C_5V^{3+}$ at the inner surface of the vesicles, in the presence of 0.1 vol % benzyl alcohol at pH 7. (●) total $C_5V^{\bullet 2+}$ concentration, measured in situ by absorbance at 633 nm; (○) outer surface $C_5V^{\bullet 2+}$ concentration, measured electrochemically; (⊙) inner surface $C_5V^{\bullet 2+}$ concentration, calculated from the total and outer surface concentrations.

where $V^{n+}$ is the oxidized viologen, $V^{(n-1)+}$ the one-electron-reduced viologen, $k_{red}$ the rate constant for photoinduced reduction, $k_{leak}$ and $k_{leak}^{-1}$ the rate constants for leaking out and penetration inside the vesicles, respectively, and $k_{reox}$ the rate constant for reoxidation at the working electrode. With the exception of $k_{red}$, these rate constants can be considered as first-order with respect to the reduced viologen concentration. Fortunately, $k_{red}$ does not need to be known for the estimation of the leaking rate constant, as shown below. The constant $k_{reox}$ was measured experimentally in units of oxidation current per mole of reduced viologen [A·L·mol$^{-1}$] or [C·s$^{-1}$·L·mol$^{-1}$] in the electrochemical cell (solution volume 0.07 L). It was converted to s$^{-1}$ by replacing moles with their Coulomb equivalent (Faraday relation) according to the following equation:

$$k_{reox}[s^{-1}] = \frac{\text{molar current } [C \cdot s^{-1} \cdot L \cdot mol^{-1}]}{\text{volume (0.07 L)}} \frac{1}{96487}[mol \cdot C^{-1}] \quad (2)$$

The constant $k_{reox}$ was dependent on the geometry and stirring conditions of the electrochemical cell, factors that were kept constant for all experiments. The overall process described in Scheme 1 corresponded to the irreversible, photostimulated extraction of the viologen from inside the vesicles. An estimation of $k_{leak}$ was obtained from the derivation of the outer surface reduced viologen concentration:

$$\frac{1}{S_{out}} \frac{d[V^{(n-1)+}]}{dt} = k_{leak}\frac{1}{S_{in}}[V^{(n-1)+}]_{in} - k_{leak}^{-1}\frac{1}{S_{out}}[V^{(n-1)+}]_{out} - k_{reox}\frac{1}{S_{out}}[V^{(n-1)+}]_{out} \quad (3)$$

where $S_{in}$ and $S_{out}$ are the inner and outer vesicle surface areas, respectively. Neglecting membrane asymmetry,[19] we assumed that $k_{leak} = k_{leak}^{-1}$ and found that

$$k_{leak} = \frac{\frac{d[V^{(n-1)+}]_{out}}{dt} + k_{reox}[V^{(n-1)+}]_{out}}{(S_{out}/S_{in})[V^{(n-1)+}]_{in} - [V^{(n-1)+}]_{out}} \quad (4)$$

The $S_{out}/S_{in}$ ratio was taken as 1.18, corresponding to spherical vesicles of 1000-Å outer diameter and 40-Å membrane thickness.[5] This is an average diameter estimated from the electron micrographs (Figure 5) and from previous data obtained with DHP vesicles.[8,18] DHP vesicles are usually larger than phospholipid vesicles.[21] The $k_{leak}$ values found for entrapped $MV^{2+}$ by using eq 4 (based on ref 6 results), for entrapped $C_5V^{3+}$ with coentrapped CdS colloids, and entrapped $C_5V^{3+}$ with externally adsorbed CdS colloids, are given in Table IV. $C_5V^{\bullet 2+}$ leaked ca. 18 times slower than $MV^{\bullet +}$ under similar conditions (inside the vesicles with coentrapped CdS colloids). It was most probably the consequence of the extra positive charge of $C_5V^{\bullet 2+}$. Charge-dependent ion permeability had also been observed in phospholipid vesicles.[21] A further reduction of the leaking rate of $C_5V^{\bullet 2+}$ by a factor 30 was found when the CdS colloids were externally adsorbed instead of being coentrapped with the viologen molecules. Physical methods revealed a partial penetration of CdS colloids into the membrane. Such a perturbation could have facilitated transmembrane diffusion of coentrapped viologens. As pointed out by a referee, this 30-fold effect could have also resulted from the development of electric potential across the membrane as inward transmembrane electron transfer took place. This potential would have opposed outward transmembrane diffusion of positively charged viologens. Both effects could, in principle, have contributed to the observed improvement of leaking behavior.

**TABLE IV: Leaking Rate Constants $k_{leak}$ of Reduced Viologens in DHP Vesicles, As Calculated with Eq 4**

| configuration | viologen molecule | $k_{leak}$ of reduced viologen, absolute, s$^{-1}$ | $k_{leak}$ of reduced viologen, relative |
|---|---|---|---|
| viologen inside, CdS inside | $MV^{2+}$ [a] | $(2.7 \pm 1.2) \times 10^{-2}$ | 540 |
| viologen inside, CdS inside | $C_5V^{3+}$ | $(1.5 \pm 0.3) \times 10^{-3}$ | 30 |
| viologen inside, CdS outside | $C_5V^{3+}$ | $(5 \bullet 1) \times 10^{-5}$ | 1 |

[a] From ref 6.

Although the kinetics of viologen reduction is a complex process that depends on the viologen, CdS colloids, and electron-donor concentrations (not to mention light intensity and other factors), an apparent first-order $k_{red}$ value can be estimated for comparative purpose. The initial slope of the total reduced viologen concentration in Figure 7, expressed in $C_5V^{\bullet 2+}$ concentration per unit time, can be divided by $C_5V^{3+}$ concentration to yield an apparent first-order rate constant. The value obtained was ca. $1.6 \times 10^{-3}$ s$^{-1}$, compared to ca. $5 \times 10^{-5}$ s$^{-1}$ for the leaking rate constant. Therefore, reduced viologen was generated ca. 30 times faster than it could leak out, which caused its accumulation inside the vesicles.

*Quantum Yields and Transmembrane Electron Transfer.* In Table II are given the 410-nm quantum yields of viologen reduction for the three studied configurations, as well as the presumed limiting factors for these quantum yields. The value of 0.4–0.6 found for the configuration with CdS colloids *and* viologens *outside* the vesicles was very close to what was found for CdS colloids in simpler aqueous media.[23] Electron–hole recombination,

(21) Lee, L. Y. C.; Hurst, J. K. *J. Am. Chem. Soc.* **1984**, *106*, 7411.

an intrinsic property of the CdS colloids, was therefore the most probable limiting factor.

The quantum yield found in the configuration with CdS colloids *and* viologens *inside* the vesicles may appear surprisingly low. However, it had been found that this quantum yield was very dependent on the electron-donor (benzyl alcohol) concentration.[6,22] In these experiments, benzyl alcohol was added externally and left to equilibrate for ca. 24 h before the illumination experiments. Nevertheless, most of the benzyl alcohol remained outside of the vesicles, as it was dissolved in water, and only a very small amount was expected to reside within the bilayer membrane or in the inner aqueous pool. The supply of electron donor necessary to maintain viologen reduction was therefore limited by its transmembrane diffusion.

When CdS colloids were located outside the vesicles (attached to the outer surface), the electron donor did not need to cross the bilayer membrane to get oxidized, regardless of where the viologens were. The lower quantum yield found when the viologens were inside compared to the case where they were outside was therefore due to the limited efficiency of *transmembrane electron transfer*. Undesired initial presence of viologen outside the vesicles in the configuration of Figure 7 could be excluded since it would have produced an electrochemical response as soon as illumination began, which was not the case.

(22) Youn, H. C.; Tricot, Y.-M.; Fendler, J. H. *J. Phys. Chem.* **1987**, *91*, 581.
(23) Henglein, A. *J. Phys. Chem.* **1982**, *86*, 2291.

## Conclusion

This work is an example of a clear differentiation between vesicular transmembrane electron transfer and transmembrane molecular diffusion. It showed that redox-induced leaking, a problem that can affect similar experiments using the popular methylviologen or its derivatives, could be controlled by synthetic modification of the redox compound. Leakproof energy storage during a time of practical significance was achieved with a viologen derivative having only one extra *positive* charge. The present results have demonstrated the potential of combined in situ electrochemical and spectrophotometric techniques for the description of complex phenomena in vesicular systems.

*Acknowledgment.* We thank Dr. Y. Marikovski, Membrane Research Department, Weizmann Institute of Science, for taking the electron micrographs.

**Registry No.** $MVCl_2$, 1910-42-5; DHP, 2197-63-9; $(C_5N)Br$, 15008-33-0; (EtV)Br, 39127-05-4; $(C_5V)Br_3$, 131588-24-4; $(C_5V)Br_4$, 131588-25-5; CdS, 1306-23-6; benzyl alcohol, 100-51-6; 1,5-dibromopentane, 111-24-0; trimethylamine, 75-50-3; 4,4'-bipyridine, 553-26-4; ethyl bromide, 74-96-4.

# Crystal-Plane-Specific Effect of Promoters on Active Sites of $V_2O_5$ Catalyst

**Atsushi Satsuma,* Akio Furuta,† Tadashi Hattori, and Yuichi Murakami**

*Department of Synthetic Chemistry, School of Engineering, Nagoya University, Furo-cho, Chikusa-ku, Nagoya 464, Japan, and Kinu-ura Research Department, JGC Corporation, Sunosaki-cho, Handa, Aichi 475, Japan*
*(Received: April 3, 1990; In Final Form: November 16, 1990)*

Crystal-plane-specific effect of the promoters on the active sites of $V_2O_5$ catalysts has been investigated by using model catalysts which selectively expose the (010) plane of $V_2O_5$ on $TiO_2$ followed by calcination under optimum condition. Addition of $P_2O_5$, $WO_3$, $MoO_3$, and $SnO_2$ to the 010 catalyst did not cause any changes in its structure as confirmed by various characterization methods: XRD, IR, SIMS, and XPS. After the addition of the promoters, the surface concentration of the V=O species on 010 catalysts did not increase. However, in the case of conventionally mixed $V_2O_5$ catalysts which expose various crystallographic planes, the V=O species remarkably increased. It was concluded that the increase in the surface concentration of V=O species on the mixed catalysts is not caused by the promoting effect on the (010) plane, but on the other planes.

## Introduction

It is well-known that the catalytic properties depend on the crystallographic plane exposed on the surface. In metal catalysts, it has been verified that catalysis differs on different metal planes,[1-7] and studies on crystal-plane-specific catalysis have been performed by using a single crystal of metal.[8] Crystal plane specificity can be assigned to the surface-active sites depending on the configuration of metal atoms, such as kink and step sites. According to Blakely and Somorjai,[3] step sites on platinum are the active sites for C-H and H-H bond breaking processes, while kinks are effective for C-C bond scission.

In the case of metal oxide catalysts, a few studies also have been devoted to the crystal-plane-specific reaction. Volta et al.[9] investigated the oxidation of alkenes over a pure $MoO_3$ crystal and showed that the (100) plane is active and selective for the allylic oxidation, while the (010) plane is nonselective. Ziolkowski et al.[10] also investigated the catalysis of crystals using pure $MoO_3$ and a solid solution of $Mn_{1-x}\phi_xV_{2-2x}Mo_{2x}O_6$. In these studies, the crystal-plane-specific catalysis was ascribed to the specific active oxygen species on the plane, such as Mo-O species. A good correlation was obtained between activity and bond strength of the species. Such investigations are less advanced in metal oxides than those in metal catalysts.

† JGC Corporation.

(1) McAllister, J.; Hansen, R. S. *J. Chem. Phys.* **1973**, *59*, 414.
(2) Löffler, D. G.; Schmidt, L. D. *J. Catal.* **1976**, *41*, 440; *Surf. Sci.* **1976**, *59*, 195.
(3) Blakely, D. W.; Somorjai, G. A. *J. Catal.* **1976**, *42*, 181.
(4) (a) Nieuwenhuys, B. F.; Somorjai, G. A. *J. Catal.* **1977**, *46*, 259. (b) Salmeron, M.; Gale, R. J.; Somorjai, G. A. *J. Chem. Phys.* **1977**, *67*, 5324. (c) Spencer, N. D.; Schoonmaker, D. C.; Somorjai, G. A. *Nature* **1981**, *294*, 643. (d) Gillespie, W. D.; Herz, R. K.; Petersen, E. E., Somorjai, G. A. *J. Catal.* **1981**, *70*, 147. (e) Somorjai, G. A.; Zaera, F. *J. Phys. Chem.* **1982**, *86*, 3070.
(5) Dalami-Imelik, G.; Massardien, *Proc. 6th Int. Congr. Catal.* **1977**, 90.
(6) (a) Goodman, G. W. *Surf. Sci* **1982**, *123*, L 679. (b) Kelley, R. D.; Goodman, D. W. *Surf. Sci.* **1982**, *123*, L 743; Campell, C. T.; Goodman, D. W. *Surf. Sci.* **1982**, *123*, 413.
(7) Herz, R. K.; Gillespie, W. D.; Petersen, E. E.; Somorjai, G. A. *J. Catal.* **1981**, *67*, 371.
(8) (a) Ertl, G. In *Catalysis Science & Technology*; Anderson, J. R., Boudart, M., Eds.; Springer-Verlag: New York, 1983; Vol. 4, Chapter 3. (b) Maire, G., Garin, F. G., *Ibid.* **1983**, Vol. 6, Chapter 3. (c) Campbell, C. T. *Adv. Catal.* **1989**, *36*, 1.
(9) Volta, J. C.; Desquesnes, W.; Moraweck, B.; Coudurier, G. *React. Kinet. Catal. Lett.* **1979**, *12*, 241. Tatibouet, J. M.; Germain J. E.; Volta, J. C. *J. Catal.* **1983**, *82*, 240. Volta, J. C.; Tatibouet, J. M.; Phichitkul, C.; Germain, J. E. *Proc. 8th Int. Congr. Catal.* **1984**, *4*, 451. Volta, J. C.; Tatibouet, J. M. *J. Catal.* **1985**, *93*, 467.

0022-3654/91/2095-3248$02.50/0 